Biomaterials 33 (2012) 1135–1145

Contents lists available at SciVerse ScienceDirect

Biomaterials

journal homepage: www.elsevier.com/locate/biomaterials

Intracellular pathways and nuclear localization signal peptide-mediated gene transfection by cationic polymeric nanovectors

Qinglian Hu [a], Jinlei Wang [a], Jie Shen [a], Min Liu [a], Xue Jin [a], Guping Tang [a,b,**], Paul K. Chu [b,*]

[a] Institute of Chemical Biology and Pharmaceutical Chemistry, Zhejiang University, Hangzhou 310028, PR China
[b] Department of Physics & Materials Science, City University of Hong Kong, Tat Chee Avenue, Kowloon, Hong Kong, China

ARTICLE INFO

Article history:
Received 27 September 2011
Accepted 10 October 2011
Available online 8 November 2011

Keywords:
Polyethylenimine (PEI) - cyclodextrin (CyD)
Cell internalization
Lysosomal trafficking
Nuclear signal peptide

ABSTRACT

Polyethylenimine (PEI) - based polymers are promising cationic nanovectors. A good understanding of the mechanism by which cationic polymers/DNA complexes are internalized and delivered to nuclei helps to identify which transport steps may be manipulated in order to improve the transfection efficiency. In this work, cell internalization and trafficking of PEI-CyD (PC) composed of β-cyclodextrin (β-CyD) and polyethylenimine (PEI, Mw 600) are studied. The results show that the PC transfected DNA is internalized by binding membrane-associated proteoglycans. The endocytic pathway of the PC particles is caveolae- and clathrin-dependent with both pathways converging to the lysosome. The intracellular fate of the PC provides visual evidence that it can escape from the lysosome. Lysosomal inhibition with chloroquine has no effect on PC mediated transfection implying that blocking the lysosomal traffic does not improve transfection. To improve the nuclear delivery of PC transfected DNA, nuclear localization signal (NLS) peptides are chosen to conjugate and combine with the PC. Compared to PC/pDNA, PC-NLS/pDNA, and PC/pDNA/NLS can effectively improve gene transfection in dividing and non-dividing cells.

1. Introduction

Non-viral gene delivery systems are promising in gene therapy because of the capacity for large genes, immunogenicity, and tissue-specific targeting [1,2]. PEI-based non-viral gene delivery vectors have tremendous potential [3,4] and several non-viral vectors are currently under development [5]. The potential barriers to the translocation of exogenous DNA from outside the cell to the nucleus include cell binding, internalization, endosomal escape, and nuclear entry [6]. Binding of vectors to the cell surface is a prerequisite to subsequent internalization, and membrane-associated proteoglycans play an important role in polycation-mediated cell binding [7]. Endocytosis is currently considered the primary method in which non-viral gene delivery vectors are internalized [8], although some reports have suggested that non-viral gene delivery has a non-endocytic mechanism [9]. There are multiple endocytic pathways including phagocytosis as well as clathrin- and caveolae-dependent endocytosis [10,11], but recent studies have failed to demonstrate the dominance of any particular internalization processes that lead to transfection. Thus, further studies of the uptake and trafficking mechanisms are required to design vectors. Nuclear import of pDNA limits the transfection efficiency of non-viral vectors. As transfected DNA is too large to be passively transported, it must either be actively transported through nuclear pores or diffuse into the nucleus while the nuclear membrane is disassembled during cell division [12–14]. The mechanism governing the translocation of cationic polymers/DNA complexes into nuclei is not well understood and remains an important area of investigation in order to improve non-viral gene therapy. The nuclear localization signal (NLS), which is recognized by nuclear protein, can efficiently transfer macromolecules into the nucleus from cytoplasm by active transport [13], and the application of NLS peptides for non-viral gene transfer has been investigated [15–17].

We have previously reported a PEI-based polymer composed of low molecular weight PEI (600 Da) cross-linked by β-cyclodextrin (β-CyD) molecules (PEI600-CyD, PC) [18]. PC is biodegradable and displays high transfection efficiency in culture neurons. Moreover, folic acid [19], TAT-R8 [20], and MC-10 oligopeptide [21] have been grafted on PC. They exhibit higher targeting and transfection efficiency as well as low cytotoxicity in various tumor cell lines and different mouse models. Recently, low-dose Dox was cross-linked to PC to produce multifunctional PC-Dox pro-drug to carry p53

* Corresponding author. Tel.: +86 852 34427724; fax: +86 852 34420542.
** Corresponding author. Institute of Chemical Biology and Pharmaceutical Chemistry, Zhejiang University, Hangzhou 310028, PR China. Tel./fax: +86 571 88273284.
E-mail addresses: tangguping@zju.edu.cn (G. Tang), paul.chu@cityu.edu.hk (P.K. Chu).

0142-9612/$ – see front matter © 2011 Elsevier Ltd. All rights reserved.
doi:10.1016/j.biomaterials.2011.10.023

plasmid in the form of PC-Dox/p53 complexes to treat multi-drug resistant breast cancers. Furthermore, the cancer therapeutic effects of drug and gene therapies have been investigated [22]. In this study, PEI-CyD (PC) is used as a model and by monitoring the intracellular fate of PC, we can determine whether DNA is transported to lysosomes and if so, whether utilizing lysosomotrophic agents such as chloroquine which prevents the activity of lysosomal enzymes can improve gene transfection. Furthermore, the effects of the cell cycle on PC mediated gene transfection and gene transfection of PC/pDNA, PC-NLS/pDNA, and PC/pDNA/NLS in dividing and non-dividing cells are investigated. Our objective is to study the cell binding and internalization mechanism of non-viral vectors. It is a key step in gene transfection and this study is also of practical significance concerning the application of cationic polymers to gene and drug delivery.

2. Material and methods

2.1. Chemicals and peptides

Polyethylenimine (PEI, MW 25 KDa and MW 600Da), β-cyclodextrin (MW 1135), fluorescent lectin wheat germ agglutinin (FL-WGA), and lectin wheat germ agglutinin (L-WGA) were acquired from Vector Laboratories (Burlingame, CA, USA). Amiloride hydrochloride, filipin, chlorpromazine hydrochloride, n-succinimidyl-3-(2-pyridyldithiol) propionate (SPDP, MW312.37), 3-(4,5-dimethylthiazol-2-yl)-2,5-

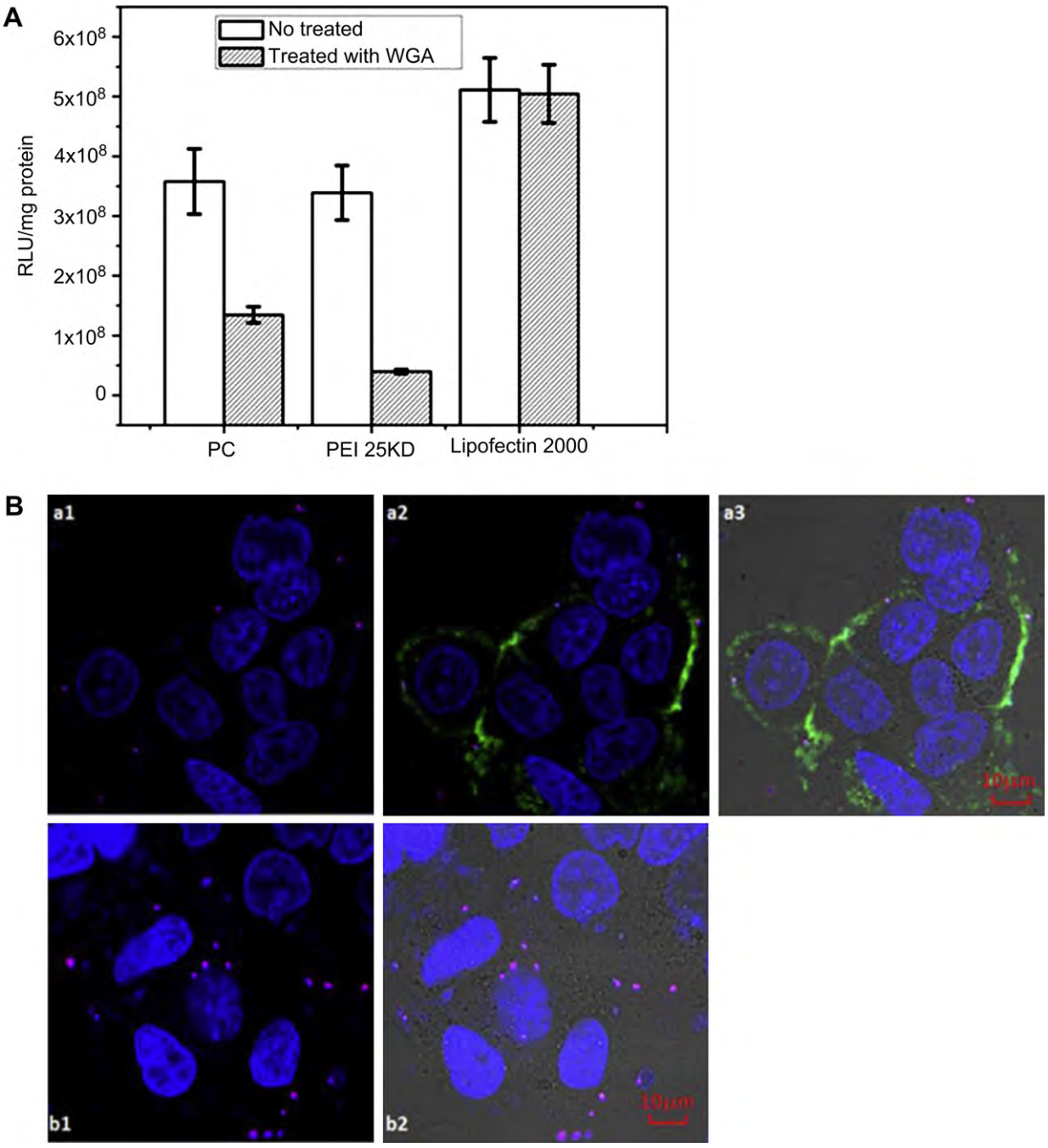

Fig. 1. Transfection efficiency (A) and cell uptake of PC/pDNA (B) in CACO-2 cells with and without the treatment of WGA. The transfection efficiencies are showing as means ± SD ($n = 3$). The Hochest nuclear stain is shown in blue, CX-rhodamin labeled plasmid in red, and FL-WGA in green. (For interpretation of the references to colour in this figure legend, the reader is referred to the web version of this article.)

diphenyl tetrazolium bromide (MTT), and chloroquine were purchased from Sigma–Aldrich (St. Louis, MO, USA). Digitonin was obtained from Calbiochem (La Jolla, CA, USA) and 1,1-carbonyldiimidazole (CDI) was purchased from Pierce (Rockford, USA). Lyso-Tracker-Red and Hochest 33342 were purchased from the Beyotime Institute of Biotechnology (Haimen, Jiangsu, China), whereas NLS1 (PKKKRKVEDPYC) and NLS2 (PKKKRKVPKKKRKVEDPYC) were purchased from GL Biochem (Shanghai, China).

2.2. Cell culture and transfection

The HEK293 cells were cultured in Dulbecco's modified eagle medium (DMEM) containing 10% bovine serum (FCS), whereas the B16BL6 cells were cultured in RPMI 1640 containing 10% bovine serum (FCS) and CACO-2 cells in RPMI 1640 containing 20% fetal bovine serum (FBS). In the luciferase transfection experiments, the cells of interest were seeded with a density of 3×10^4/well in 48-well plates and grown for 18 h at 37 °C in a humidified 5% CO_2 incubator. The medium was replaced with 0.3 ml of fresh serum-free medium, and 100 ml of freshly prepared vectors/pDNA complex containing 1 μg of DNA was added to each well. The transfection experiments with Lipofectin2000 were performed according to the manufacturer's instructions. To achieve optimal transfection efficiency, the N/P ratios of the PEI25KD and PC were 10 and 25, respectively. After 4 h of transfection, the medium was replaced by fresh growth medium and then the cells were incubated for an additional 24 h. Finally, the cells were washed twice with PBS and harvested to test the Luciferase activity according to standard protocols of the luciferase assay system (Promega). The total protein was measured using a BCA protein assay kit (Pierce).

WGA was used to test the blocking of cationic polymer binding to CACO-2 cells [23]. The cells were pretreated with 50 μg/ml WGA for 30 min at room temperature, washed with PBS, and then transfected with the complexes for 4 h. In the temperature-dependent transfection experiments, the CACO-2 cells were incubated at 4 and 37 °C for 1 h and then transfected at the same temperature for 4 h. Endocytic inhibitors were used to identify the possible endocytotic pathways and the following concentrations were selected based on previous studies [20]: 20 mM amiloride, 1 μg/ml filipin, and 10 μg/ml chlorpromazine. The cells were pretreated with the inhibitors for 30 min at 37 °C and then transfected with complexes for 4 h at 37 °C in the presence of the inhibitors. The cells were washed with PBS and cultured in fresh media in the absence of the inhibitors for another 24 h prior to measuring the luciferase activity. In the Chloroquine experiments, the cells were transfected in the presence of 100 mM chloroquine for 4 h. The cells were washed with PBS and cultured in fresh media without chloroquine for another 24 h prior to measurement of the luciferase activity.

Gene transfection of growth-arrested cells is conducted according to the following procedures. 5×10^4/well cells were seeded into 48-well plates and grown for 24 h to achieve full confluence. Subsequently, the medium was removed, the cells were washed with PBS, and serum-free medium was added to each well for 24 h. The cells were transfected with complexes for 4 h. In order to inhibit nuclear pore transport, the cells were permeabilized with digitonin for 5 min in ice and washed

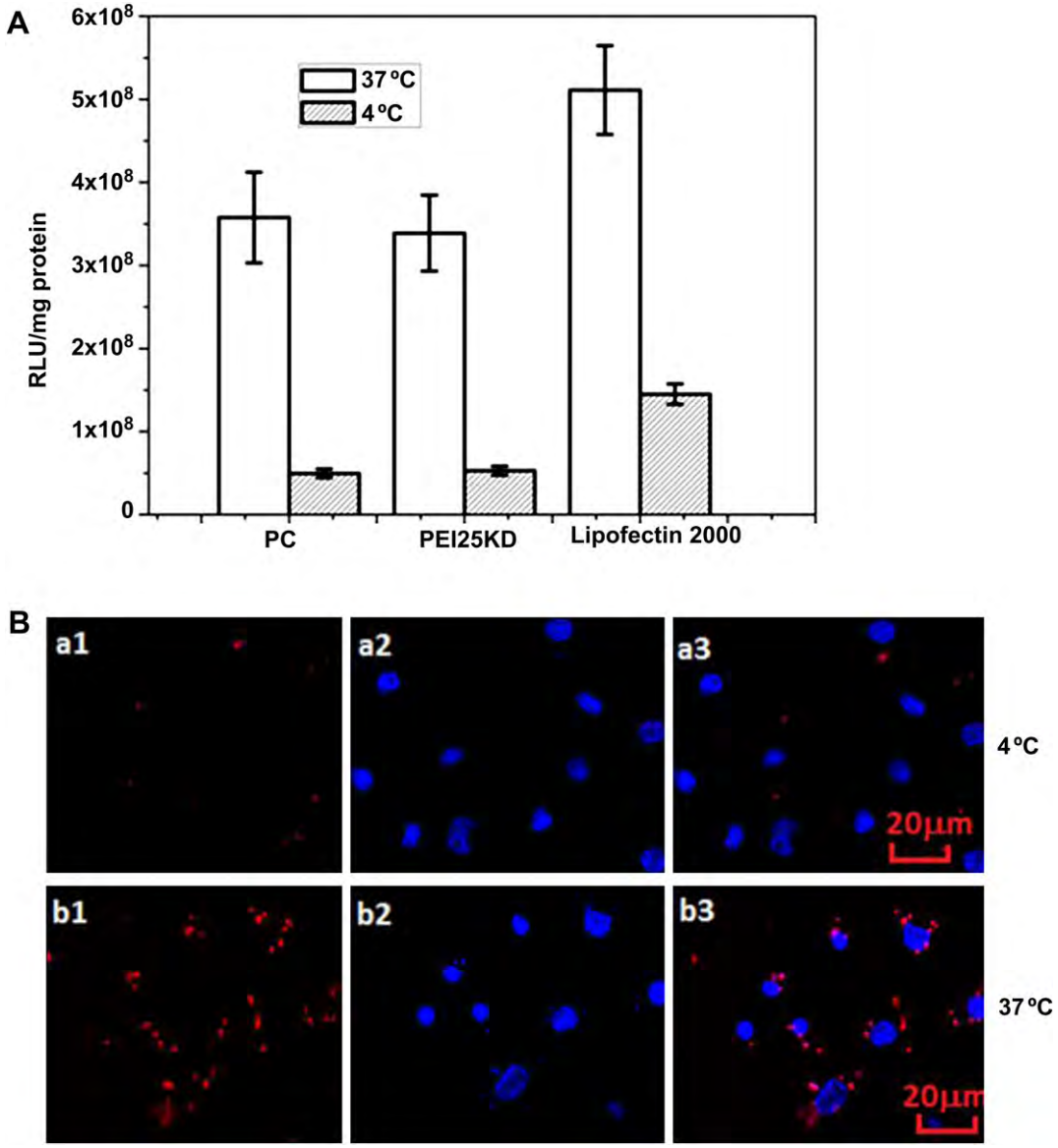

Fig. 2. (A) Transfection efficiency and (B) cell uptake of PC/pDNA in CACO-2 cells at 4 and 37 °C. The transfection efficiencies are showing as means ± SD ($n = 3$). The nuclei are stained with hoechest 3325 and the plasmid is labeled by CX-rhodamin.

with PBS. The cells were then treated with WGA for 30 min and washed with PBS. The cells were transfected with complexes for 4 h. In the EGFP plasmid transfection experiments, the HEK293 cells were cultured and transfected as described above. The percentages of EGFP expressing cells and mean fluorescence intensity (MFI) were employed to quantify the transfection efficiency by means of flow cytometry. After transfection for 36 h, the cells were trypsinized, washed, and re-suspended in the PBS buffer, and the EGFP positive cells were tested by flow cytometry (Caliber, CA, USA). The untransfected HEK293 cells were used to set the background.

2.3. Fluoresence labeling

The plasmid DNA was labeled by the Label IT Tracker™ Nucleic Acid Labeling Kits, CX-Rhodamine (Mirus) according to the provided protocol. In brief, the plasmid DNA and label IT reagents were mixed and incubated at 37 °C for 1 h. Any unreacted labeling reagent was removed and the plasmid DNA was purified by ethanol precipitation. The FITC-conjugated PC was obtained by adding 50 mg of PC to 2.5 μmol of the FITC isomer solubilized in 5 mL of a 1:1 DMSO/water mixture. The solution was stirred in the dark for 2 h at room temperature. The unreacted FITC molecules were removed by dialysis (molecular weight cut off 8000) in distilled water for 2 days and the products were then lyophilized.

2.4. Inhibition of cell uptake

Cell internalization inhibition was examined by confocal microscopy. 5×10^4/well CACO-2 cells were seeded onto 24-well plates and grown for 18 h. 1 μg of CX-rhodamine labeled pDNA was complexed with PC and then transfected with cells as described above. After transfection for 2 h, the cells were fixed with fresh 4% paraformaldehyde and then treated with 10 μg/ml hoechest33245 in PBS for 10 min. The confocal images were acquired on a confocal scanning laser microscope (CLSM, Radiance 2100, Bio-Rad).

2.5. Intracellular trafficking of PC

5×10^4/well CACO-2 cells were seeded onto 24-well plates and grown for 18 h. The transfected FITC-PC/pDNA complexes used in the chloruquine experiments and transfection medium contained 100 mM chloroquine. At specific time points during transfection or post-transfection, the cells were rinsed and incubated in the medium containing 100 nm Lyso-tracker Red for 1 h. The cells were fixed with fresh 4% paraformaldehyde and then treated with 10 μg/ml hoechest33245 in PBS for 10 min. The confocal images were taken on a confocal scanning laser microscope (CLSM, Radiance 2100, Bio-Rad).

2.6. Cell cycle analysis

HEK293, B16BL6, and CACO-2 cells were seeded into 6-well plates with a density of 2×10^5/well and grown for 24 h to achieve full confluence. After the medium was removed, the cells were washed with PBS, and serum-free medium was added to each well for 24 h. The controls were seeded into 6-well plates with a density of 3×10^5/well and grown for 24 h to achieve full confluence. Cell cycle analysis was performed using the cell cycle kit (Beyotime). The cells were trypsinized, washed, and fixed by 75% ethanol at −20 °C overnight. The cell suspension was washed and re-suspended in 100 μl of PBS, and then RNaseA and propidium iodide were added and incubated at 37 °C for 30 min. The fluorescence-stained cells were analyzed by flow cytometry (Caliber, CA, USA).

2.7. Polymer synthesis and biochemical characterization

The PC backbone was synthesized by a previously reported protocol [18]. The PC (100 mg) was dissolved in 10 ml of PBS and SPDP (2.5 mg, 0.01 mmol) was dissolved in a mixture of 0.5 ml PBS and 0.5 ml DMSO. The two solutions were mixed and 0.1 ml of triethylamine was added. The mixture was stirred in the dark for 2 h. The nuclear signal peptides NLS1 (8.27 mg, 5.55 nmol) or NLS2 (11.81 mg, 5.55 nmol) were dissolved in 1 ml of PBS buffer and added slowly to the solution under stirring in the dark for another 4 h. The mixtures were dialyzed with a dialysis tube (MW 8000-14000) for 2 days and then freeze dried for further use. The conjugations of NLS1 onto the PC backbone were confirmed by ^{1}H NMR. The particle size and zeta-potential measurements were conducted at 25 °C by dynamic light scattering (DLS) on the Zetasizer 3000 (Malvern Instruments, Worcestershire, UK). The morphology of the complexes was examined by field-emission scanning electron microscopy (FE-SEM, JEOL JSM-7400F, Japan) at an accelerating voltage of 6.0 kV. 5 μL of the complexes were placed on a silicon plate which was carbon-taped to the sample holder and air-dried prior to conducting SEM.

2.8. Nuclear trafficking of vectors/pDNA

Prior to confocal microscopy, the HEK293 cells were seeded with a density of 6×10^4/well in the confocal imaging dishes (Glass Bottom microwells, MatTek Corp., Ashland, MA). 2 μg of the Rhodamine-labeled plasmid DNA was mixed with the polymers/pDNA and treated in the cells in the absence of serum. After 4 h of incubation at 37 °C, the cells were incubated for 6 h in the DMEM medium (10% FCS). Afterwards, the cells were fixed with fresh 4% paraformaldehyde and treated with 10 μg/ml hoechest33245 in PBS for 10 min. Localization of the labeled pDNA in the cells was examined by confocal laser scanning microscopy (CLSM, Radiance 2100, Bio-Rad).

3. Results and discussion

Binding of vectors to the cell surface is prerequisite to internalization. It is well known that cell surface proteoglycans have a significant impact on polycation-mediated gene delivery [7]. Sialic acid as a component of glycoproteins is involved in the binding and transport of positively charged molecules due to their negative charge [24,25] and has been reported as a receptor for virus infection [26]. The wheat germ agglutinin (WGA) lectin which has a strong affinity to N-acetyl-glucosamine and sialic acid has been utilized to block cationic polymers from binding to CACO-2 cells [23]. When WGA is pre-incubated with CACO-2 cells for 30 min, the gene expression mediated by PC and PEI25KD is 36% and 12%, respectively of those of the untreated cells, but no significance difference can be found from lipofectin2000 (Fig. 1A). Confocal microscopy is employed to examine the trafficking of pDNA transfected by PC. The pDNA is labeled by CX-rhodamine (red

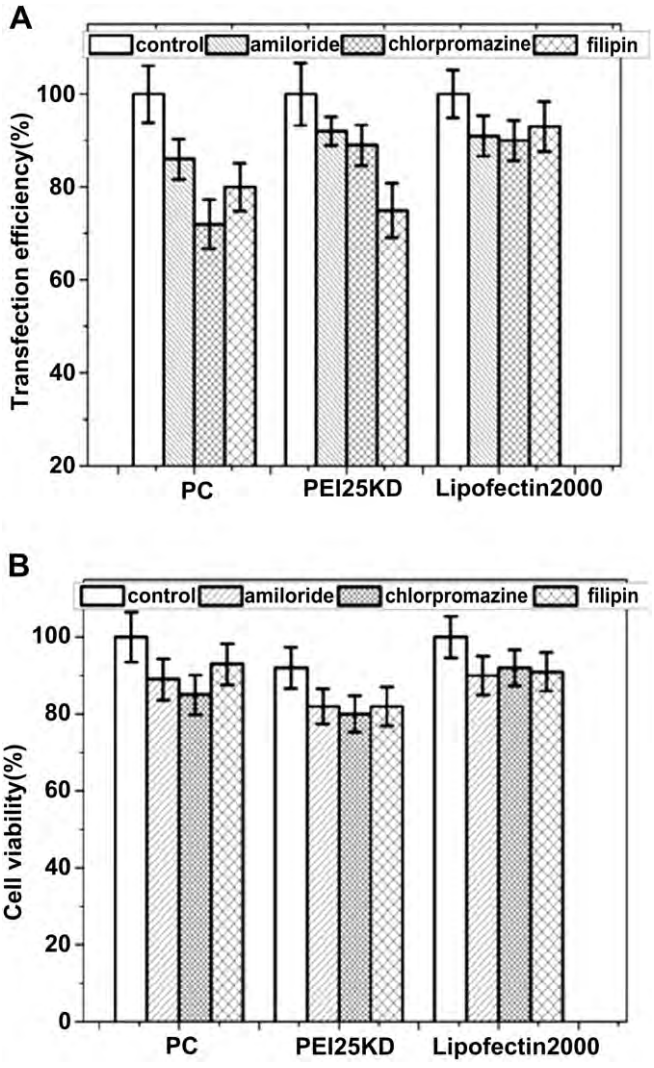

Fig. 3. (A) Transfection efficiency and (B) cell viability of CACO-2 cells treated with specific endocytic inhibitors. The data are shown as means ± SD ($n = 3$).

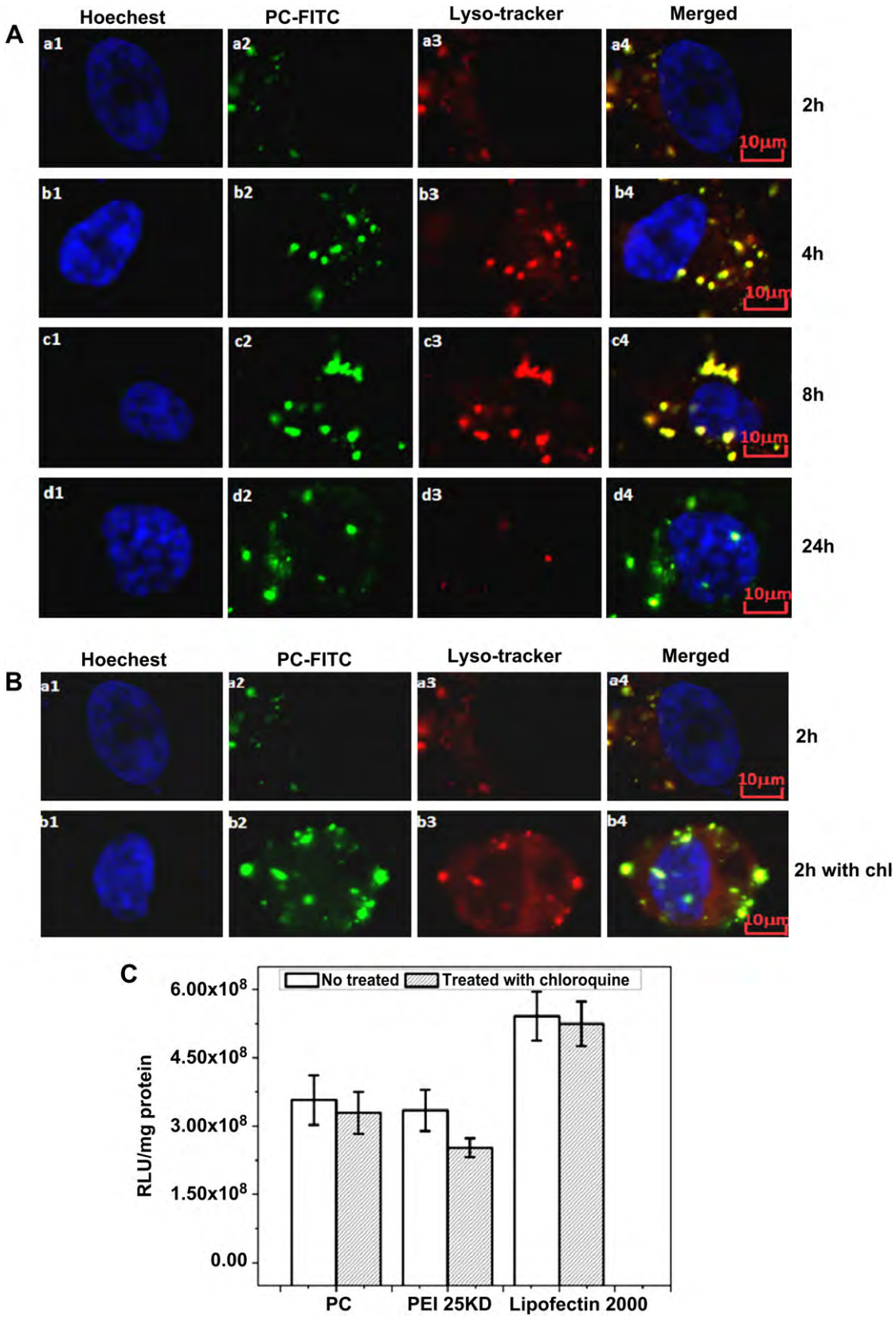

Fig. 4. (A) Intracellular fate and cytoplasmic release of PC in CACO-2 cells at different time point, (B) Confocal fluoresence image, and (C) Transfection efficiency (C) of CACO-2 cells with and without chloriquine. The transfection efficiencies are showing as means ± SD ($n = 3$). The Hochest nuclear stain is shown in blue, lysosome in red (Lyso-Tracker), and PC-FITC in green. (For interpretation of the references to colour in this figure legend, the reader is referred to the web version of this article.)

fluorescence) whereas the nuclei are stained with Hoechst 33342 (blue fluorescence). FL-WGA interacts with the cell membrane (green fluorescence). As shown in Fig. 1B, with regard to the pre-incubated WGA with CACO-2 cells, pDNA diminishes in the cell membrane compared to the untreated WGA (Fig. 1B, a3 and b2). This indicates that polyplexes and lipoplexes have different cell binding and for polyplexes, sialic acid may act as a receptor facilitating cell binding. Compared to PEI25KD, PC shows lower inhibition after the WGA treatment implying that the PC interacts with the cell membrane mainly *via* binding sialic acid and diversified cell binding is involved.

It is important to define the internalization pathways for the non-viral vectors that lead to efficient functional transfection. The cells are pre-incubated at 4 °C to completely inhibit energy dependent cellular uptake. Temperature dependent gene transfection is conducted to examine the internalization of PC, PEI25KD, and Lipofectin2000 in the CACO-2 cells. The transfection efficiency is greatly reduced at 4 °C mediated by PC (~86%), PEI25KD (~85%) and Lipofectin2000 (~70%), as depicted in Fig. 2A. Internalization of the fluorescence-labeled plasmid DNA/PC complexes at 4 and 37 °C is observed visually. Fig. 2B shows that at 4 °C, it is difficult to observe red fluorescence around the cell (Fig. 2B, a3), but at 37 °C, the large amount of red spots reflects the labeled plasmids inside the cells (Fig. 2B, b3). The results indicate that endocytosis is the main way of PC and PEI25KD internalization. With regard to lipofectin2000, it enters cells *via* a combination of non-endocytotic and endocytotic pathways [27].

Transfection experiments with specific endocytic inhibitors are performed to elucidate the endocytic pathways. Filipin inhibits the raft/caveolae pathway, chlorpromazine inhibits clathrin-mediated endocytosis, and amiloride inhibits macropinocytosis [28]. As shown in Fig. 3A, treating the CACO-2 cells with chlorpromazine and filipin results in 28% and 20% decrease in PC mediated gene transfection, whereas treatment with amiloride reduces gene transfection by 14%. Hence, the PC internalizes *via* a combination of caveolae - and clathrin − dependent endocytosis, with the latter endocytic pathway contributing more substantially. With regard to PEI25KD, amiloride and chlorpromazine decrease gene transfection slightly, whereas filipin reduces it by 25%. Therefore, the internalization pathway of PEI25KD depends largely on the caveolae pathway [29]. The three endocytic inhibitors show no obvious effects on Lipofectin2000 mediated gene transfection (Fig. 6 A) and

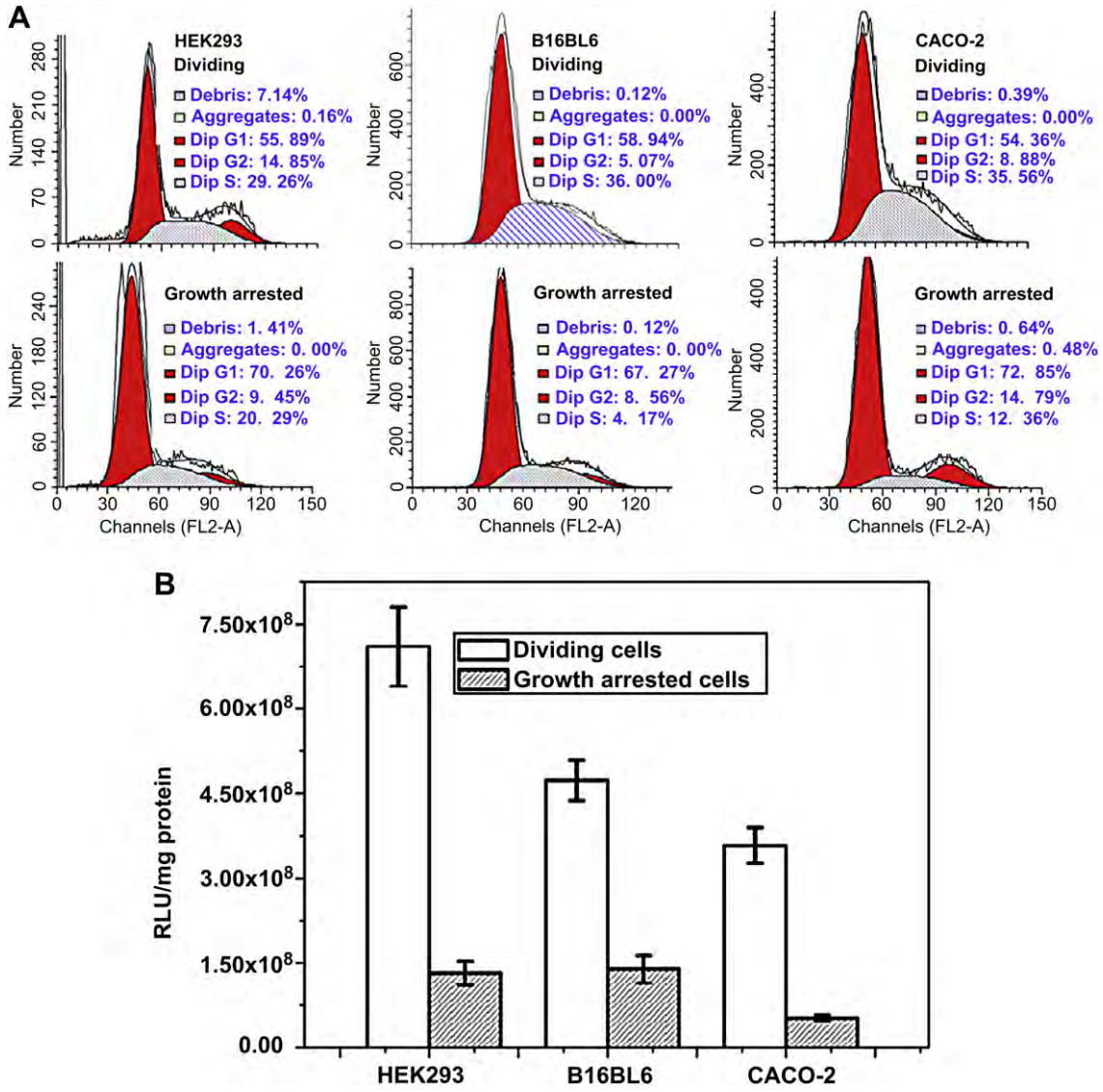

Fig. 5. (A) Cell cycle analysis and (A) Transfection efficiency of dividing and growth-arrested cells. The data are shown as means ± SD ($n = 3$).

lipoplexes undergo an internalization pathway different from that of the polyplexes. The cell viability shows that the toxicity of the inhibitors does not influence the gene expression under the experimental conditions (Fig. 3B).

Lysosomal degradation of transfected DNA has been proposed to be a major reason for poor transfection efficiency [30]. Here, we determine the intracellular fate of PC and associated gene transfection. The FITC-PC/pDNA complexes are incubated with CACO-2 cells which are monitored for 24 h by confocal microscopy. The lysosomes are stained with Lyso-Tracker (red fluorescence). As shown in Fig. 4A, 2 h after transfection, a small number of FITC-PC tracks the lysosome, as evidenced by colocalization of FITC-PC and lysosome (Fig. 4A, a4). PC fluorescence and Lyso-Tracker staining are more intense after 4 h or 8 h than 2 h transfection (Fig. 4A, b4 and c4), suggesting that PC accumulation in the lysosome is time dependent. After 24 h, PC-FITC escapes in significant quantities from the lysosomal membrane and enters the cytoplasm (Fig. 4A, d4). Hence, PC tracking is time dependent and it is able to escape from the lysosome. The contributor is PEI which has a high buffering effect due to the presence of protonated amine groups in the structure that increases the osmotic pressure in the endosome resulting in disruption of the endosomal membrane [31]. These results also indicate that PC tracked to lysosome and lysosomotrophic agents such as chloroquine [32] can be utilized to determine whether preventing the activity of lysosomal enzyme can improve gene transfection. Confocal microscopy is used to examine

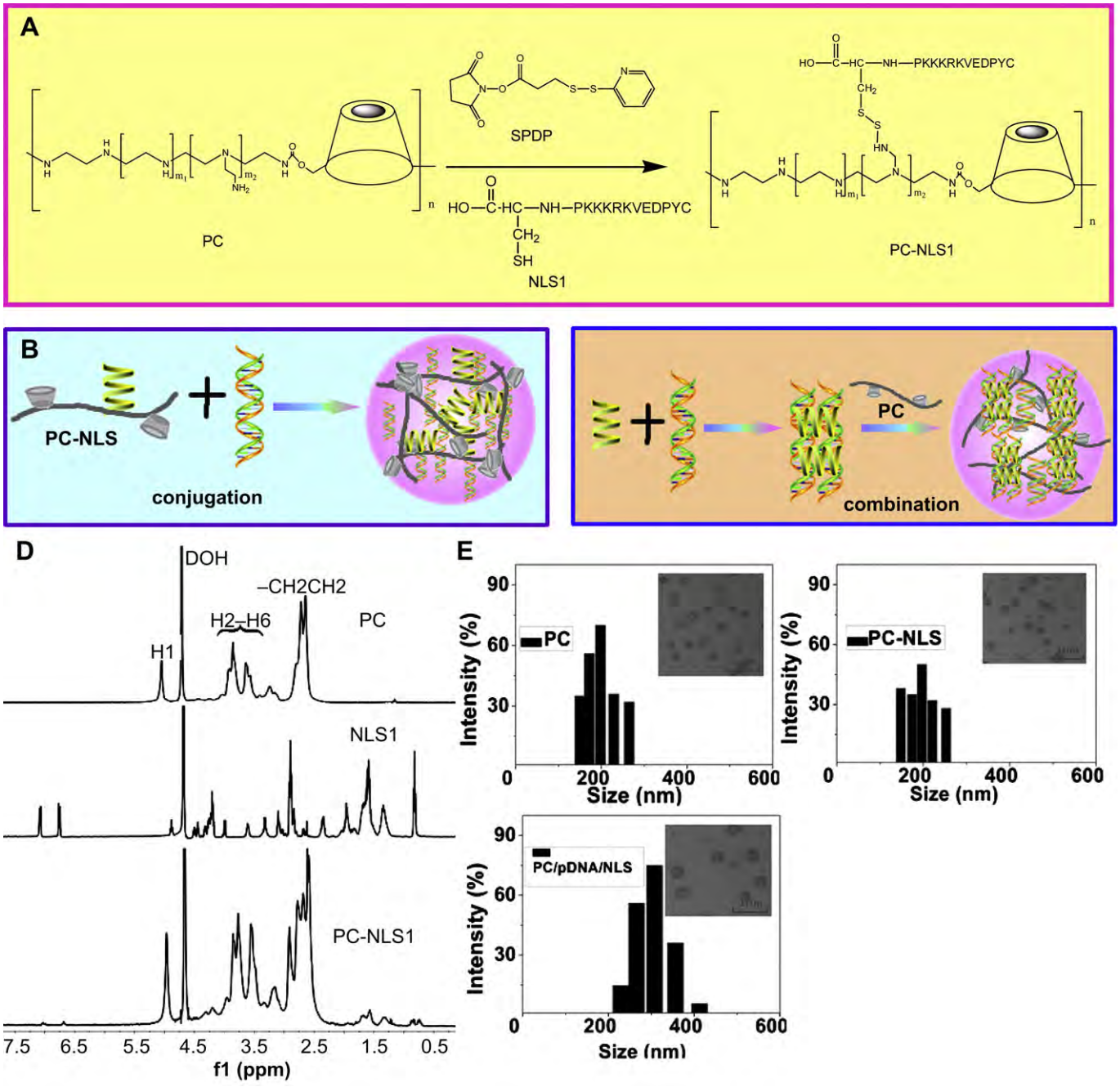

Fig. 6. (A) Synthesis of PC-NLS1, (B) Schematic diagram of plasmid DNA encapsulated PC-NLS1, (C) PC/pDNA/NLS as a nano-sized DNA carrier, ^{1}H MNR spectra of PC, NLS1, PC-NLS1 in D_2O (D). The size distribution of the vectors/pDNA is measured by DLS and the inset images present the SEM images of the vectors/pDNA in (E).

Table 1
Summary of cell cycles of dividing and growth arrested cells.

Cell cycle Cell lines	G1 (%)	S (%)	G2 (%)	G2/G1 (%)
Dividing HEK293	55.89	29.26	14.85	1.92
Growth arrested HEK293	70.26	20.29	9.45	1.98
Dividing B16BL6	58.94	38	5.07	1.95
Growth arrested B16BL6	67.27	24.17	8.65	1.95
Dividing CACO-2	54.56	36.56	8.88	1.85
Growth arrested CACO-2	72.85	12.36	14.79	1.90

the intracellular distribution of PC with and without chloroquine in the CACO-2 cells. As shown in Fig. 4B, after incubation for 2 h, a large amount of PC-FITC is released from the lysozyme into the cytoplasm (Fig. 4B, b4). A small amount of PC-FITC is trapped in the lysosome without chloroquine, as evidenced by colocalization of green fluorescence and red fluorescence (Fig. 4B, a4). The luciferase activity of PC, PEI25KD, and lipofectin2000 after treatment with chloroquine reveals that chloroquine has no effects on gene transfection (Fig. 4C). Lysosomal trafficking fails to improve transfection and nuclear translocation of plasmid appears to a limiting step in transfection.

Compared to viral gene vectors, non-viral vectors have relatively low transfection efficiency, and inefficient transfer of DNA from the cytoplasm to the nucleus has been identified as a major reason, particularly in postmitotic and quiescent cells where there is no periodic breakdown in the nuclear membrane [12,14]. A good understanding of the mechanism governing PC mediated nuclear entry will enable improvement in PC based gene delivery strategies. In this work, the influence of the cell cycle on gene transfection is studied using dividing and growth-arrested cells by serum starvation. The standard flow cytometric analysis of propidium iodide-stained cells confirms that serum-starved HEK293, B16BL6, and CACO-2 cells are predominantly (70%, 68%, and 73%) in the G0/G1 phase of the cell cycle (Fig. 5A and Table 1). In these three cell lines, the luciferase activity decreases by 80%, 70% and 85%, respectively (Fig. 5B). The nuclear entry of pDNA mediated by polyplexes is mainly *via* the breakdown of the nuclear membrane during mitosis [33]. However, the gene expression also occurs in the growth-arrested cells, suggesting that the PC/pDNA complexes or free plasmid DNA can cross the nuclear envelope.

It is unclear whether improving the active nuclear transport will benefit PC mediated gene transfection in dividing and growth-arrested cells. However, it is known that NLS can improve the nuclear entry and enhance the gene transfection of non-viral vectors [15,17,34]. Two different lengths of NLS peptides are selected to conjugate and combine to the PC (Fig. 6). The conjugations of NLS1 onto the PC backbone were assessed by ^{1}H NMR. As shown in Fig. 6D, the protons at δ 4.9 ppm are assigned to the H6 hydroxyl group inside the ring of CD, those at δ 2.3–2.8 ppm correspond to –CH2–CH2-N from PEI600, and those at δ 7.0 ppm are associated with the aromatic group of the NLS. The characteristic peaks of NLS can be observed from PC-NLS1, indicating that the NLS peptide is indeed conjugated to the PC backbone. The samples are also analyzed by UV–visible spectrophotometry. The UV spectrum of PC-NLS is similar to that of NLS but displays a bathochromic shift attributable to modification of the NLS between the free and conjugated states (data not shown).

Table 2
Particle size and zeta potentials of PC, PC-NLS, and PC/pDNA/NLS.

	Particle size (nm)	Zeta potentials
PC	191 ± 8	29 ± 1.32
PC-NLS1	195 ± 11	20.6 ± 2.2
PC-NLS2	185 ± 9	19.6 ± 1.3
PC/pDNA/NLS (1/0.1/0.01)	296 ± 7	10.2 ± 0.15
PC/pDNA/NLS (1/0.1/0.1)	307 ± 12	9.4 ± 0.52
PC/pDNA/NLS (1/0.1/1)	450 ± 22	5.8 ± 0.42
PC/pDNA/NLS (1/0.1/10)	680 ± 52	2.8 ± 0.42

The physicochemical properties such as morphology, size, and zeta potential of the complexes are important parameters which influence the cellular uptake. The size and zeta potential of PC/pDNA, PC-NLS/pDNA, and PC/pDNA/NLS complexes are listed in Table 2. Compared to the PC/DNA complexes, the PC-NLS1/DNA and PC-NLS2/DNA complexes at N/P of 25 have similar particle size and zeta potential values (190 nm and 20 mV). The particle size of PC/pDNA/NLS increases whereas the zeta potential decreases (Fig. 6E). Scanning electron microscopy (SEM) discloses that most of the

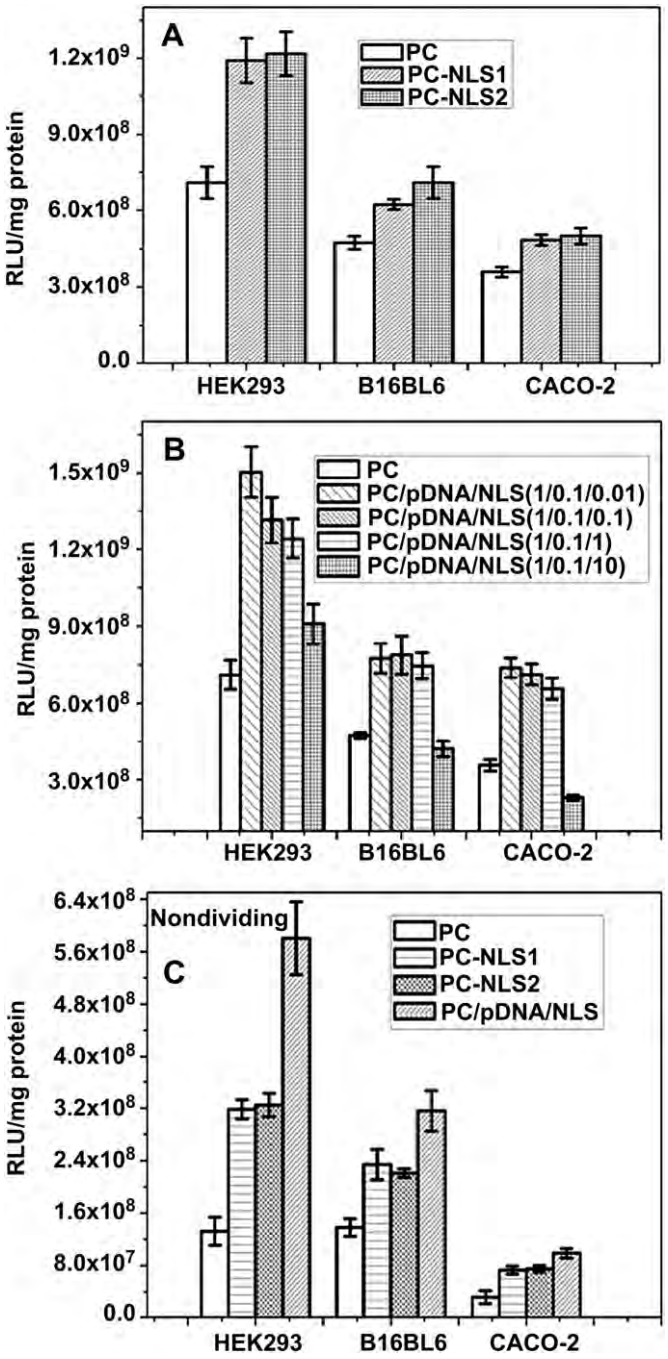

Fig. 7. (A) Transfection efficiency of conjugation, (B) Combination vectors/pDNA in dividing cell lines, and (C) Transfection efficiency of conjugation and combination vectors/pDNA in growth-arrested cells. The data are shown as means ± SD (n = 3).

particles have the form of spherical aggregates. The size discrepancy observed between the PC-NLS/pDNA and PC/pDNA/NLS complexes indicates that addition of NLS disrupts PC condensed pDNA and the DNA perhaps absorbs onto the surface of the PC/pDNA/NLS complexes. The cytotoxicity of the complexes is evaluated by the MTT assay. The PC/pDNA, PC-NLS/pDNA, and PC/pDNA/NLS complexes exhibit lower cytotoxicity for the three cells lines compared to the PEI25KD/pDNA complexes (data not shown).

In vitro gene transfection of PC-NLS/pDNA is performed using HEK293, B16BL6, and CACO-2 cells lines to determine the optimal conditions for transfection. Among the three cell lines, PC-NLS5 (NLS and PC feed ratio of 5%) shows the highest levels of gene expression at N/P 25 (data not shown). As shown in Fig. 7A, PC-NLS1 and PC-NLS2 enhance gene transfection by 1.5–2 folds compared to PC, and so PC-NLS can enhance gene transfection. To ensure the bioactivity of NLS, the PC/pDNA/NLS complexes are prepared. Using the

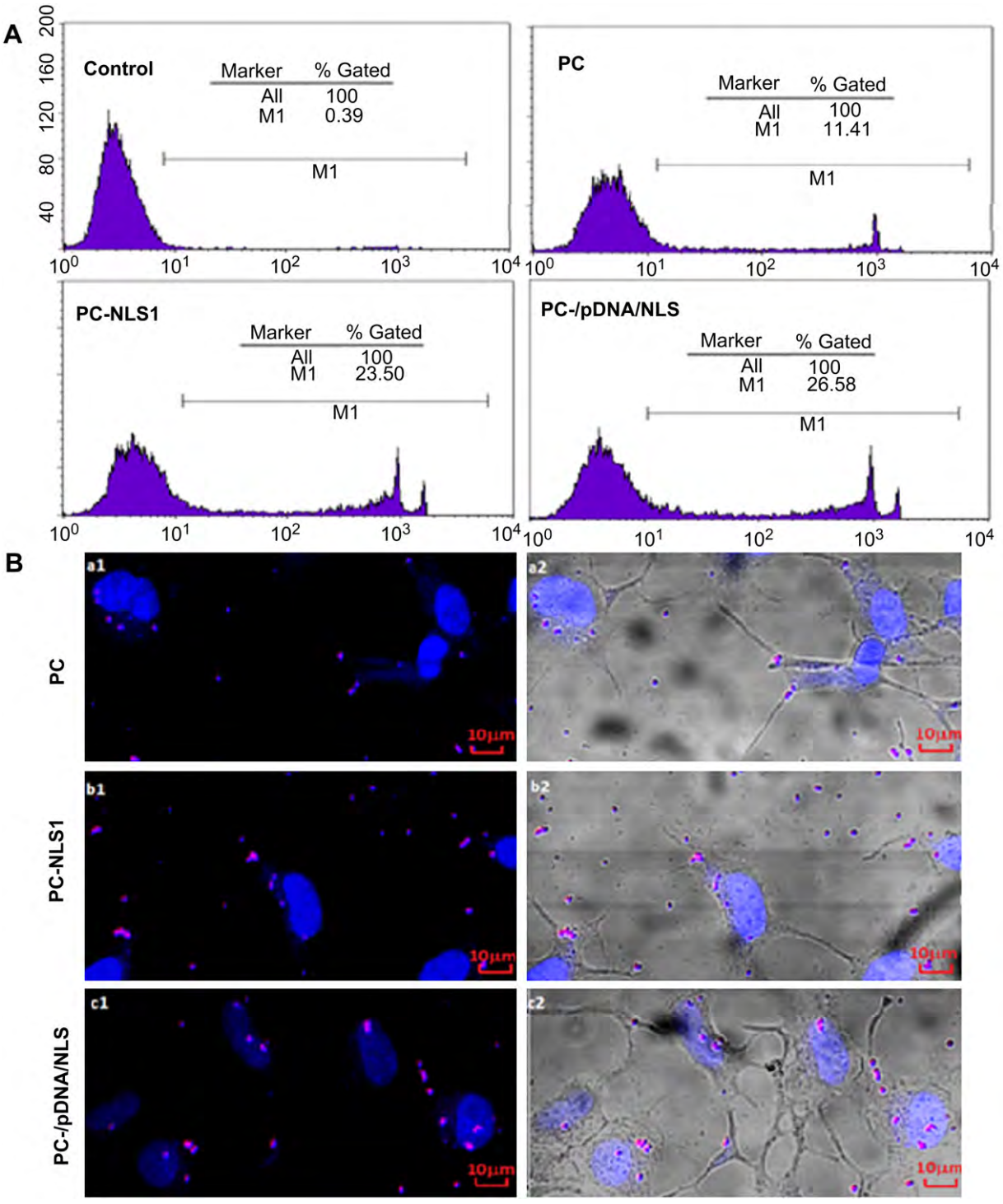

Fig. 8. (A) Flow cytometry analysis and (B) Traces of the labeled pDNA at 6 h post-transfection in HEK293 transfected by PC, PC-NLS1, and PC/pDNA/NLS. The N/P is 25. The Hochest nuclear stain is shown in blue and CX-rhodamin labeled plasmid in red. (For interpretation of the references to colour in this figure legend, the reader is referred to the web version of this article.)

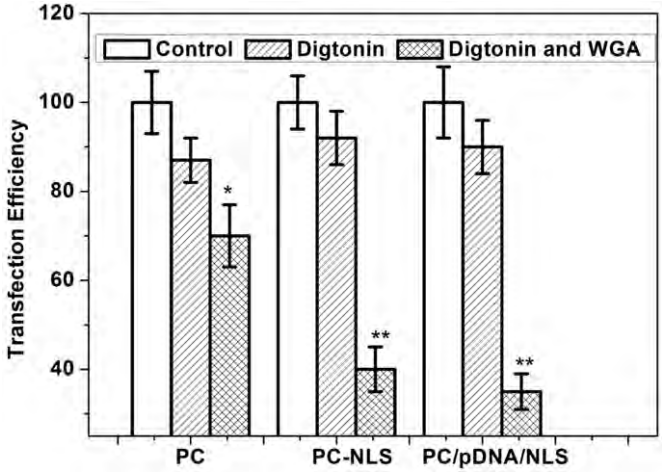

Fig. 9. Inhibition of luciferase expression treated with digitonin and WGA in CACO-2 cells. The data are shown as means ± SD ($n = 3$).

optimal N/P ratio of PC/pDNA of 25, different ratios of NLS are added to the complexes (Fig. 7B). The transfection efficiency is influenced by the ratio of NLS. The optimal ratio of PC/pDNA/NLS is 1/0.1/0.01 (w/w/w) which yields the highest transfection efficiency. It is about 3 times larger than that of PC but the transfection efficiency diminishes if the NLS is further increased. At a weight ratio of 1/0.1/10 (w/w/w), the gene expressions are smaller than those of the PC. This means excess NLS weakens the electrostatic interactions between the PC and pDNA and also disrupts PC condensation pDNA into tight complexes (Table 2). Thus, the weight ratio of 1/0.1/0.01 (PC/pDNA/NLS) is chosen in the following study. To minimize NPC-independent nuclear transport that occurs when the nuclear membrane is decreased during mitosis, growth-arrested cells are used to evaluate gene expression. The contribution of NLS to the transfection efficiency is studied in non-dividing HEK293, B16BL6, and CACO-2 cells. The gene transfection efficiency of PC-NLS1/pDNA and PC/pDNA/NLS at an N/P ratio of 25 is about 2.5 and 5 times higher than that of PC in the HEK293 cells, 1.5 and 3 folds of that in the B16BL6 cells, and 2.5 and 3 folds of that in the CACO-2 cells (Fig. 7C). The contribution of NLS to the transfection efficiency in non-dividing cells is greater than that in dividing cells. In dividing cells, nuclear delivery of pDNA can be achieved when the nuclear membrane is decreased during mitosis. However, in non-dividing cells, pDNA transfer between the cytoplasm and nucleus requires a nuclear localization signal (NLS).

It is further confirmed by flow cytometry analysis of the HEK293 cells (Fig. 8A). The percentages of green fluorescence positive cells transfected with PC-NLS1 and PC/pDNA/NLS are 2.1 and 2.3 times higher than those of PC. These results are consistent with those obtained from the luciferase experiments and present evidence that the NLS-based vectors can improve gene transfection in dividing cells. The ability of PC, PC-NLS, and PC/NLS to transport plasmid DNA to the cytoplasm and nucleus in the HEK293 cells is evaluated by confocal laser scanning microscopy. As shown in Fig. 8B, after 6 h of incubation, PC-NLS and PC/pDNA/NLS can deliver the plasmid to the nucleus (Fig. 8B, b1, b2, and c1, c2), whereas PC only delivers the plasmid to the perinuclear

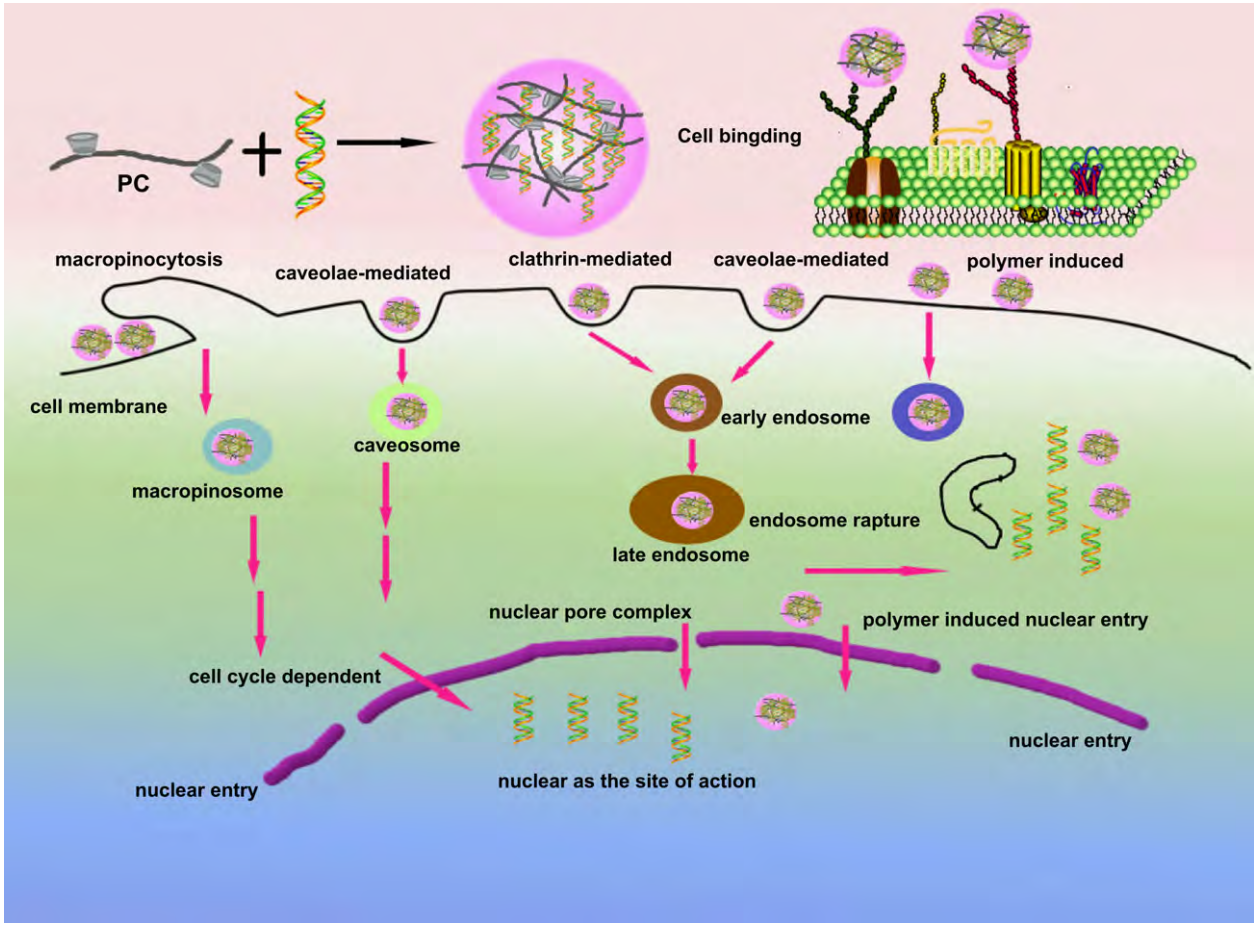

Fig. 10. Schematic illustration of the process of gene delivery mediated by PC.

region of the cytoplasma (Fig. 8B, a1, a2). Hence, the NLS-based vectors facilitate translocation of pDNA to the nucleus and the results are in agreement with the transfection efficiency. The nuclear import assay and WGA blockage are utilized to explore the nuclear transfer of NLS-based pDNA delivery involving the nuclear pore complex. The digitonin-permeabilized cells are used to examine nuclear protein import and export. The detergent digitonin selectively permeabilizes membranes rich in cholesterol, such as the plasma membrane, while leaving intact membranes of intracellular organelles with low levels of cholesterol such as the nucleus and secretory granules [35]. In the digitonin-permeabilized cells, WGA can specifically bind with nuclear pore complexes (NPC). Digitonin has a small negative effect on gene transfection mediated by PC, PC-NLS, and PC/NLS in the CACO-2 cells, suggesting that the permeabilized cells do not facilitate PC mediated gene transfection. As shown in Fig. 9, after treatment with digitonin and WGA, the luciferase expression is reduced by 30%, 60% and 70%, respectively as transfected by PC, PC-NLS, and PC/NLS. Hence, NLS mediated nuclear transport is involved in the nuclear pore complex.

Fig. 10 depicts the mechanism of the intracellular trafficking of cationic polymers such as PC involving the successive steps of cationic polymers interacting with cell membrane *via* binding membrane-associated proteoglycans (step 1) and through clathrin- and caveolae -dependent endocytic pathway to enter the cells (step 2). The endocytotic vesicles grow in number, colocalize with lysosome (step 3), and escape from the lysosome (step 4). Cell cycle dependent nuclear entry is a critical determinant which governs the transfection effectiveness and the NLS peptides can improve the nuclear entry of DNA and consequently enhance gene transfection.

4. Conclusion

PC transfected DNA is internalized *via* binding membrane-associated proteoglycans. The endocytic pathway of the PC particles is caveolae- and clathrin-dependent with both pathways converging to the lysosome. The intracellular fate of the PC indicates that it can escape from the lysosome. Lysosomal inhibition with chloroquine has no effect on PC mediated transfection implying that blocking the lysosomal traffic does not improve transfection. To improve the nuclear delivery of the PC transfected DNA, nuclear localization signal (NLS) peptides are chosen to conjugate and combine to the PC. Compared to PC/pDNA, PC-NLS/pDNA and PC/pDNA/NLS can effectively improve gene transfection in dividing and non-dividing cells.

Acknowledgements

This work was jointly supported by the National High Technology Development Program of China (863 Program 2007AA03Z355, 2009AA02Z416), National Natural Science Foundation of China (grant # 30970711 and 21074111), the key project of International Science and Technology Corperation (grant # 2011DFA30790), (CityU 9231026 and CityU 9678028), and Hong Kong Research Grants Council (RGC) General Research Funds (GRF) # CityU 112510.

References

[1] Luo D, Saltzman WM. Synthetic DNA delivery systems. Nat Biotechnol 2000; 18:33–7.
[2] Huard J, Li Y, Peng H, Fu FH. Gene therapy and tissue engineering for sports medicine. J Gene Med 2003;5:93–108.
[3] Park TG, Jeong JH, Kim SW. Current status of polymeric gene delivery systems. Adv Drug Deliv Rev 2006;58:467–86.
[4] Boussif O, Lezoualc'h F, Zanta MA, Mergny MD, Scherman D, Demeneix B, et al. A versatile vector for gene and oligonucleotide transfer into cells in culture and in vivo: polyethylenimine. Proc Natl Acad Sci U S A 1995;92:7297–301.
[5] Guo X, Huang L. Recent advances in nonviral vectors for gene delivery. Acc Chem Res; 2011. DOI: 10.1021/ar200151m.
[6] Wiethoff CM, Middaugh CR. Barriers to nonviral gene delivery. J Pharm Sci 2003;92:203–17.
[7] Mislick KA, Baldeschwieler JD. Evidence for the role of proteoglycans in cation-mediated gene transfer. Proc Natl Acad Sci U S A 1996;93:12349–54.
[8] Khalil IA, Kogure K, Akita H, Harashima H. Uptake pathways and subsequent intracellular trafficking in nonviral gene delivery. Pharmacol Rev 2006;58: 32–45.
[9] Felgner PL, Gadek TR, Holm M, Roman R, Chan HW, Wenz M, et al. Lipofection: a highly efficient, lipid-mediated DNA-transfection procedure. Proc Natl Acad Sci U S A 1987;84:7413–7.
[10] Conner SD, Schmid SL. Regulated portals of entry into the cell. Nature 2003; 422:37–44.
[11] Rejman J, Conese M, Hoekstra D. Gene transfer by means of lipo- and polyplexes: role of clathrin and caveolae-mediated endocytosis. J Liposome Res 2006;16:237–47.
[12] Pouton CW, Wagstaff KM, Roth DM, Moseley GW, Jans DA. Targeted delivery to the nucleus. Adv Drug Deliv Rev 2007;59:698–717.
[13] van der Aa MA, Mastrobattista E, Oosting RS, Hennink WE, Koning GA, Crommelin DJ. The nuclear pore complex: the gateway to successful nonviral gene delivery. Pharm Res 2006;23:447–59.
[14] Lam AP, Dean DA. Progress and prospects: nuclear import of nonviral vectors. Gene Ther 2010;17:439–47.
[15] Glover DJ, Ng SM, Mechler A, Martin LL, Jans DA. Multifunctional protein nanocarriers for targeted nuclear gene delivery in nondividing cells. FASEB J 2009;23:2996–3006.
[16] Branden LJ, Mohamed AJ, Smith CI. A peptide nucleic acid-nuclear localization signal fusion that mediates nuclear transport of DNA. Nat Biotechnol 1999;17: 784–7.
[17] Bremner KH, Seymour LW, Logan A, Read ML. Factors influencing the ability of nuclear localization sequence peptides to enhance nonviral gene delivery. Bioconjug Chem 2004;15:152–61.
[18] Tang GP, Guo HY, Alexis F, Wang X, Zeng S, Lim TM, et al. Low molecular weight polyethylenimines linked by beta-cyclodextrin for gene transfer into the nervous system. J Gene Med 2006;8:736–44.
[19] Yao H, Ng SS, Tucker WO, Tsang YK, Man K, Wang XM, et al. The gene transfection efficiency of a folate-PEI600-cyclodextrin nanopolymer. Biomaterials 2009;30:5793–803.
[20] Jiang QY, Lai LH, Shen J, Wang QQ, Xu FJ, Tang GP. Gene delivery to tumor cells by cationic polymeric nanovectors coupled to folic acid and the cell-penetrating peptide octaarginine. Biomaterials 2011;32:7253–62.
[21] Huang HL, Yu H, Tang GP, Wang QQ, Li J. Low molecular weight polyethylenimine cross-linked by 2-hydroxypropyl-gamma-cyclodextrin coupled to peptide targeting HER2 as a gene delivery vector. Biomaterials 2010;31: 1830–8.
[22] Lu X, Wang QQ, Xu FJ, Tang GP, Yang WT. A cationic prodrug/therapeutic gene nanocomplex for the synergistic treatment of tumors. Biomaterials 2011;32: 4849–56.
[23] Peppas NA, Huang Y. Nanoscale technology of mucoadhesive interactions. Adv Drug Deliv Rev 2004;56:1675–87.
[24] Schauer R. Chemistry, metabolism, and biological functions of sialic acids. Adv Carbohydr Chem Biochem 1982;40:131–234.
[25] Varki A. Diversity in the sialic acids. Glycobiology 1992;2:25–40.
[26] Arnberg N, Edlund K, Kidd AH, Wadell G. Adenovirus type 37 uses sialic acid as a cellular receptor. J Virol 2000;74:42–8.
[27] Grosse S, Thevenot G, Monsigny M, Fajac I. Which mechanism for nuclear import of plasmid DNA complexed with polyethylenimine derivatives? J Gene Med 2006;8:845–51.
[28] Gabrielson NP, Pack DW. Efficient polyethylenimine-mediated gene delivery proceeds via a caveolar pathway in HeLa cells. J Control Release 2009;136: 54–61.
[29] Rejman J, Bragonzi A, Conese M. Role of clathrin- and caveolae-mediated endocytosis in gene transfer mediated by lipo- and polyplexes. Mol Ther 2005;12:468–74.
[30] Varkouhi AK, Scholte M, Storm G, Haisma HJ. Endosomal escape pathways for delivery of biologicals. J Control Release 2011;151:220–8.
[31] Lin C, Engbersen JF. Effect of chemical functionalities in poly(amido amine)s for non-viral gene transfection. J Control Release 2008;132:267–72.
[32] Ciftci K, Levy RJ. Enhanced plasmid DNA transfection with lysosomotropic agents in cultured fibroblasts. Int J Pharm 2001;218:81–92.
[33] Brunner S, Sauer T, Carotta S, Cotten M, Saltik M, Wagner E. Cell cycle dependence of gene transfer by lipoplex, polyplex and recombinant adenovirus. Gene Ther 2000;7:401–7.
[34] Opanasopit P, Rojanarata T, Apirakaramwong A, Ngawhirunpat T, Ruktanonchai U. Nuclear localization signal peptides enhance transfection efficiency of chitosan/DNA complexes. Int J Pharm 2009;382:291–5.
[35] Adam SA, Marr RS, Gerace L. Nuclear protein import in permeabilized mammalian cells requires soluble cytoplasmic factors. J Cell Biol 1990;111: 807–16.